Crystal Structure of the Novel Complex Cobalt Oxide $Sr_{0.7}Y_{0.3}CoO_{2.62}$

S. Ya. Istomin,*,† J. Grins,‡ G. Svensson,§ O. A. Drozhzhin,|| V. L. Kozhevnikov,⊥ E. V. Antipov,† and J. P. Attfield#

Department of Chemistry, Moscow State University, 119992, Moscow, Russia, Departments of Inorganic Chemistry and Structural Chemistry, Stockholm University, SE-10691, Stockholm, Sweden, Department of Materials Science, Moscow State University, 119992, Moscow, Russia, Institute of Solid State Chemistry, Ural Branch of RAS, 620219, Ekaterinburg, Russia, and Department of Chemistry, University of Cambridge, Lensfield Road, Cambridge CB2 1EW, United Kingdom

Received April 14, 2003. Revised Manuscript Received June 18, 2003

The perovskite-related crystal structure of the compound $Sr_{0.7}Y_{0.3}CoO_{2.62}$ was determined and refined using synchrotron X-ray and neutron powder diffraction, in space group $I4/mmm$, $a = 7.6237(8)$ Å and $c = 15.314(2)$ Å, to $R_I = 0.041$ in the synchrotron data set. It contains layers of CoO_6 octahedra, perpendicular to the c axis, alternating with partially disordered oxygen-deficient layers. Further characterization of the structure using electron diffraction and high-resolution electron microscopy showed that an additional superstructure was present in some of the crystallites. The structure represents a new type of layered ordering of oxygen vacancies in oxygen-deficient perovskites. Possible local atom arrangements in the oxygen-deficient layers and the structural relationship to the resembling brownmillerite-type structure for $ABO_{2.5}$ compounds are discussed.

Introduction

The oxygen content in ABO_3 compounds with perovskite-related structures can be decreased if B-cation has a stable lower oxidation state and can accept coordination numbers below six. The arrangement of the oxygen vacancies in the structures of the formed phases can be disordered or, when their concentration is high enough, ordered. In the latter category, new compounds may be found that have important physical properties, for example, layered HTSC cuprates, fast oxide ion conductors such as BIMEVOX, and so forth.

For perovskite-related oxides containing Fe or Co, ordering of oxygen vacancies yields different superstructures. The compounds $Ca_2Fe_2O_5$,[1−3] $Sr_2Fe_2O_5$,[4,5] and $Sr_2Co_2O_5$[6,7] have $ABO_{2.5}$ stoichiometries and adopt the brownmillerite ($Ca_2(Fe,Al)_2O_5$) type structure. The structures are orthorhombic with $a \approx c \approx \sqrt{2} \times a_p$ and $b \approx 4 \times a_p$, where a_p is the unit cell parameter for the cubic perovskite structure. The oxygen vacancies are ordered in a layered manner, resulting in layers with tetrahedral coordination of B-cation that alternate with octahedral ones. Other, more complicated, perovskite-related structures are found for compounds with different oxygen contents in the system $SrFeO_{3-y}$.[8] The structures of two have recently been determined using neutron powder diffraction data:[9] $Sr_4Fe_4O_{11}$ ($ABO_{2.75}$) has an orthorhombic structure with $a \approx 2 \times \sqrt{2} \times a_p$, $b \approx 2 \times a_p$, and $c \approx \sqrt{2} \times a_p$ and $Sr_8Fe_8O_{23}$ ($ABO_{2.875}$) a tetragonal one with $a \approx 2 \times \sqrt{2} \times a_p$ and $c \approx 2 \times a_p$. Structurally similar phases have been reported to form also in the systems $SrCoO_{3-y}$,[10] for example, $SrCoO_{2.80}$ with a tetragonal unit cell with $a \approx 2 \times \sqrt{2} \times a_p$ and $c \approx 2 \times a_p$, and $Sr_{1-x}Ln_xCoO_{3-\delta}$,[11] in which a tetragonal phase $Sr_{0.7}La_{0.3}CoO_{3-\delta}$ with $a \approx a_p$ and $c \approx 2 \times a_p$ has been identified on the basis of powder X-ray diffraction (XRD), electron diffraction (ED), and high-resolution electron microscopy (HREM). $RBaCo_2O_{5+y}$, R= Y, Pr, Nd, Sm, Eu, Gd, Tb, Dy, and Ho, are found to have a layered structure where oxygen atoms are removed from every second [001] plane, thus forming square pyramids around cobalt,[12−19] $a \approx a_p$ and $c \approx 2 \times a_p$. Additional

* Corresponding author. E-mail: istomin@icr.chem.msu.ru.
† Department of Chemistry, Moscow State University.
‡ Department of Inorganic Chemistry, Stockholm University.
§ Department of Structural Chemistry, Stockholm University.
|| Department of Materials Science, Moscow State University.
⊥ Institute of Solid State Chemistry, Ural Branch of RAS.
Department of Chemistry, University of Cambridge.

(1) Colville, A. A. *Acta Crystallogr. B* **1970**, *26*, 1469.
(2) Berggren, J. *Acta Chem. Scand.* **1971**, *25*, 3616.
(3) Berastegui, P.; Eriksson, S.-G.; Hull, S. *Mater. Res. Bull.* **1999**, *34*, 303.
(4) Greaves, C.; Jacobson, A. J.; Tofield, B. C.; Fender, B. E. F. *Acta Crystallogr. B* **1975**, *31*, 641.
(5) Berastegui, P.; Eriksson, S.-G.; Hull, S. *Mater. Res. Bull.* **1999**, *34*, 303.
(6) Takeda, T.; Yamaguchi, Y.; Watanabe, H. *J. Phys. Soc. Jpn.* **1972**, *33*, 970.
(7) Grenier, J.-C.; Ghobane, S.; Demazeau, G.; Pouchard, M.; Hagenmuller, P. *Mater. Res. Bull.* **1979**, *14*, 831.
(8) Takeda, Y.; Kano, K.; Yamamoto, O.; Takano, M.; Nakayama, N.; Bando, Y. *J. Solid State Chem.* **1986**, *63*, 237.
(9) Hodges, J. P.; Short, S.; Jorgensen, J. D.; Xiong, X.; Dabrowski, B.; Mini, S. M.; Kimball, C. W. *J. Solid State Chem.* **2000**, *151*, 190.
(10) Takeda, Y.; Kanno, R.; Yamamoto, O.; Takano, M.; Bando, Y. *Z. Anorg. Allg. Chem.* **1986**, *540/541*, 259.
(11) van Doom, R. H. E.; Burggraaf, A. F. *Solid State Ionics* **2000**, *128*, 65.
(12) Zhou, W.; Lin, C. T.; Liang, W. Y. *Adv. Mater.* **1993**, *5*, 735.
(13) Zhou, W. *Chem. Mater.* **1994**, *6*, 441.
(14) Martin, C.; Maignan, A.; Pelloquin, D.; Nguyen, N.; Raveau, B. *Appl. Phys. Lett.* **1997**, *71*, 1421.
(15) Akahoshi, D.; Ueda, Y. *J. Solid State Chem.* **2001**, *156*, 355.

10.1021/cm034263e CCC: $25.00
Published on Web 09/11/2003

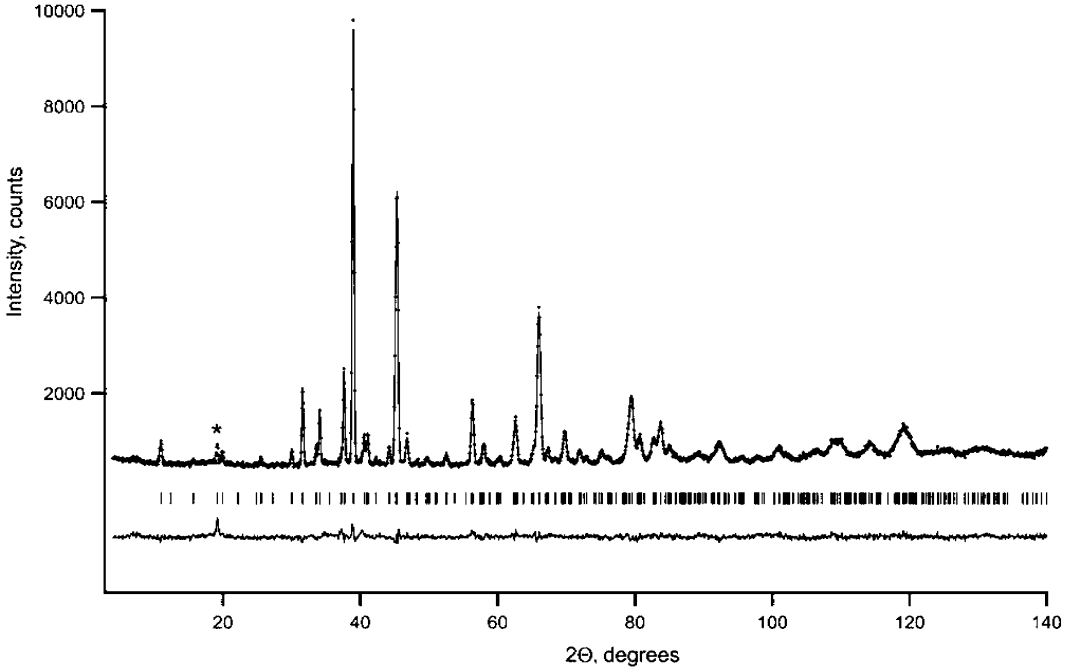

Figure 1. Observed (crosses), calculated (full line), and difference (bottom) neutron powder diffraction patterns for $Sr_{0.7}Y_{0.3}CoO_{2.62}$.

oxygens (y) are located in the vacant plane forming different types of superstructures.[15] The same type of compounds is found among ferrates; see for example ref 20. Addition of one perovskite block $BaFeO_3$ leads to the formation of ferrates $LnBa_2Fe_3O_{8+y}$, Ln = Dy, Er, and Y with a structure close to superconducting cuprate Y-123-type,[21] $a \approx a_p$ and $c \approx 3 \times a_p$.

In the course of a search for new phases in the system $Sr_{1-x}Ln_xCoO_{3-y}$, Ln = Y and Eu − Er, we have synthesized a novel compound $Sr_{0.7}Y_{0.3}CoO_{2.62}$ ($ABO_{2.62}$). It has a previously unreported type of oxygen vacancy ordering resulting in a tetragonal perovskite-related structure with $a \approx 2 \times a_p$ and $c \approx 4 \times a_p$. The refinement of the structure, using neutron and synchrotron powder diffraction data, and further characterization by ED and HREM studies, is reported here.

Experimental Section

The compound $Sr_{0.7}Y_{0.3}CoO_{2.62}$ was synthesized from stoichiometric mixtures of $SrCO_3$, Co_3O_4, and Y_2O_3. The mixtures were carefully ground and sintered in air at 1423 K for 24 h, followed by a re-grinding and further firing at 1423 K for 72 h. Thereafter, the furnace was shut off and the samples were allowed to cool to room temperature. Phase analysis of the products was made by X-ray powder diffraction photographs, recorded in a Guinier-Hägg camera with Cu $K\alpha_1$ radiation and Ge as the internal standard.

Neutron powder diffraction (NPD) data were collected at the Swedish research reactor at the NFL, Studsvik, using a wavelength of 1.47 Å, with the sample placed in a thin-walled vanadium can (i.d. = 6 mm). Synchrotron powder diffraction data were collected from a 0.4-mm-diameter capillary sample on the beamline ID31 at the ESRF, Grenoble, for 7 h with $\lambda =$ 0.40027 Å. Structure refinements were carried out using the RIETAN 2000 program.[22]

For the transmission electron microscopy (TEM) studies, small amounts of the samples were crushed in *n*-butanol. A drop of this dispersion was put on a holey carbon film supported with a copper grid. Electron diffraction (ED) studies and microanalysis were made in a JEOL JEM2000 FX instrument, operated at 200 kV and equipped with a LINK AN10000 energy-dispersive X-ray (EDX) microanalysis system. HREM studies were made in a JEOL JEM3010 UHR microscope, operated at 300 kV. Additional EDX analysis of the metal composition, on the same samples as were used for TEM, were also performed using a JEOL JSM 880 scanning electron microscope equipped with a windowless LINK *Isis* EDX system. Simulated HREM images were calculated using MacTempas.[23]

Iodometric titration was used to determine the oxygen content in the as-prepared $Sr_{0.7}Y_{0.3}CoO_{3-y}$ sample. About 50 mg of the sample under investigation was placed in a flask containing 20 mL of a 20% water solution of KI. Several drops of concentrated HCl were then added to the solution and the flask was kept in a dark place until the entire sample had dissolved. The released elementary iodine was titrated by a standard $Na_2S_2O_3$ solution with starch added as an indicator.

Results

Structure Refinements. An XRD single-phase sample was obtained for the nominal composition $Sr_{0.7}Y_{0.3}CoO_{3-y}$. The oxygen content was determined by iodometric titration to be $Sr_{0.7}Y_{0.3}CoO_{2.62}$. The EDX analyses, using both SEM and TEM, confirmed the metal composition to equal the nominal one within the esd's of the analyses. The formal oxidation state for Co is accordingly +2.94. The Guinier-Hägg powder pattern

(16) Maignan, C.; Martin, A.; Pelloquin, D.; Nguyen, N.; Raveau, B. *J. Solid State Chem*. **1999**, *142*, 247.
(17) Troyanchuk, I. O.; Kasper, N. V.; Khalyavin, D. D.; Szymczak, H.; Szymczak, R.; Baran, M. *Phys. Rev. Lett.* **1998**, *80*, 3380.
(18) Troyanchuk, I. O.; Kasper, N. V.; Khalyavin, D. D.; Szymczak, H.; Szymczak, R.; Baran, M. *Phys. Rev. B* **1998**, *58*, 2418.
(19) Vogt, T.; Woodward, P. M.; Karen, P.; Hunter, B. A.; Henning, P.; Moodenbaugh, A. R. *Phys. Rev. Lett*. **2000**, *84*, 2969.
(20) Karen, P.; Woodward, P. M. *J. Mater. Chem*. **1998**, *9*, 789.
(21) Karen, P.; Kjekshus, A.; Huang, Q.; Lynn, J. W.; Rosov, N.; Natali Sora, I.; Karen, V. L.; Mighell, A. D.; Santoro, A. *J. Solid State Chem*. **1998**, *136*, 21.
(22) Izumi, F.; Ikeda, T. *Mater. Sci. Forum* **2000**, *198*, 321.
(23) Roar Kilaas, MacTempas, www.totalresolution.com.

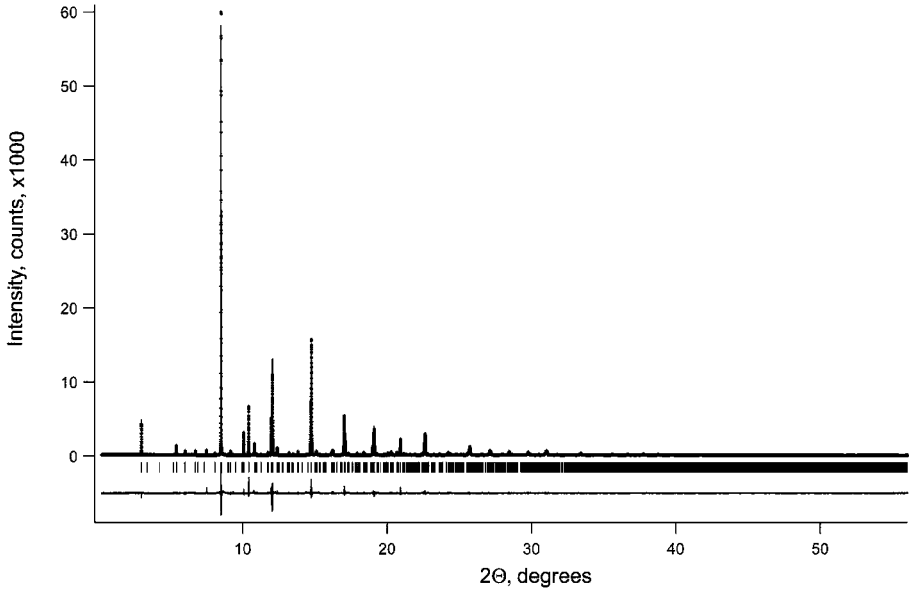

Figure 2. Observed (crosses), calculated (full line), and difference (bottom) synchrotron X-ray powder diffraction patterns for $Sr_{0.7}Y_{0.3}CoO_{2.62}$.

Table 1. Crystal and Refinement Data for $Sr_{0.7}Y_{0.3}CoO_{2.62}$ Based on the Synchrotron Data; Data for the NPD Refinement Are Bracketed

space group	*I*4/*mmm*
lattice parameters:	
a/Å	7.62389(1) (7.6193(8))
c/Å	15.32701(5) (15.313(2))
Z	16
2θ range, step	0.20 ≤ 2θ ≤ 56.05, 0.001 (4 ≤ 2θ ≤ 140, 0.08)
λ, Å	0.40027 (1.47)
R_I[a]	0.041 (0.035)
S	1.91 (1.46)
R_{wp}	0.013 (0.053)
R_p	0.094 (0.039)
number of reflections	1816 (330)
number of refined parameters	39

[a] Definitions of the criteria of fit is given in Ref. X: Izumi, F., Young, R. A., Eds. *The Rietveld Method, IUCr Monographs on Crystallography*; Oxford University Press: Oxford, 1993; Vol. 5, Chapter 13, p 22.

of $Sr_{0.7}Y_{0.3}CoO_{2.62}$ could be indexed with an *I*-centered tetragonal unit cell with unit cell parameters a = 7.6237(8) Å and c = 15.314(2) Å. The cell is related to the cubic perovskite subcell parameter a_p by $a \approx 2 \times a_p$ and $c \approx 4 \times a_p$. The synchrotron data, but neither the Guinier-Hägg nor the neutron data set, showed a few, very weak reflections from a trace amount of Y_2O_3 in the sample. The reflections from $Sr_{0.7}Y_{0.3}CoO_{2.62}$ did not reveal additional symmetry elements, implying the possible space groups to be *I*4/*mmm* (139), or its subgroups $I\bar{4}2m$ (121), $I\bar{4}m2$ (119), *I*4*mm* (107), *I*4/*m* (87), $I\bar{4}$ (82), and *I*4 (79). No additional superstructure reflections were observed in any of the powder patterns.

The positions of metal and oxygen atoms were derived by trial and error, by testing structural models in various tetragonal space groups and cell origin choices. The trial refinements supported the presumption that the structure contains layers of CoO_6 octahedra, perpendicular to the *c*-axis, that alternate with oxygen-deficient layers with cobalt atoms in CoO_4 tetrahedra. Furthermore, these refinements strongly indicated the presence of a mirror plane, perpendicular to the *c*-axis and through the cobalt and oxygen atoms in the oxygen-deficient layer. A satisfactory fit between observed and calculated intensities was obtained, both for neutron and synchrotron data, using the most symmetric tetragonal space group *I*4/*mmm*. A Legendre polynomial with 12 coefficients was used to describe the background for the NPD and synchrotron powder diffraction patterns. The peak profiles for the corresponding patterns

Table 2. Atomic Parameters for $Sr_{0.7}Y_{0.3}CoO_{2.62}$ from Synchrotron Data (Upper Values) and Neutron Data (Lower Values)

atom	site	*x*	*y*	*z*	B_{iso} (Å^2)	occ.
Sr1/Y1	4e	0	0	0.87856(8)	1.16(2)	0.7/0.3
		0	0	0.8805(7)	1.6(2)	
Sr2/Y2	8g	0	1/2	0.86701(5)	0.81(1)	0.7/0.3
		0	1/2	0.8669(4)	0.7(1)	
Sr3/Y3	4e	0	0	0.35037(6)	0.74(2)	0.7/0.3
		0	0	0.3502(5)	1.0(2)	
Co1	8h	0.7483(1)	0.7483	0	1.07(2)	1
		0.746(1)	0.746	0	1.4(2)	
Co2	8f	1/4	3/4	1/4	0.43(1)	1
		1/4	3/4	1/4	0.5[a]	
O1	16n	0	0.2493(7)	0.2330(2)	0.79(5)	1
		0	0.2422(6)	0.2395(3)	0.69(8)	
O2	16m	0.2905(3)	0.2905	0.1176(2)	1.52(7)	1
		0.2876(4)	0.2876	0.1165(3)	1.8(1)	
O3	8i	0	0.7240(8)	0	1.8(1)	1
		0	0.722(1)	0	1.7(2)	
O4	8j	0.387(2)	1/2	0	0.2(3)	1/4
		0.399(3)	1/2	0	1.6(5)	0.23(1)

[a] Not refined.

Table 3. Selected Interatomic Distances (Å) for $Sr_{0.7}Y_{0.3}CoO_{2.62}$[a]

octahedron			Sr1/Y1−O1	(×4)	2.630(4)
Co2−O1	(×4)	1.9122(2)	Sr1/Y1−O3	(×4)	2.809(4)
Co2−O2	(×2)	2.076(3)	Sr1/Y1−O2	(×4)	3.132(3)
			Sr2/Y2−O1	(×2)	2.518(5)
			Sr2/Y2−O3	(×2)	2.659(4)
			Sr2/Y2−O2	(×4)	2.728(4)
tetrahedron/ trigonal bipyramid					
Co1−O2	(×2)	1.850(3)	Sr2/Y2−O1	(×2)	2.7407(5)
Co1−O3	(×2)	1.9282(8)	Sr3/Y3−O2	(×4)	2.312(3)
Co1−O4	(×1)	2.156(7)	Sr3/Y3−O4	(×1)	2.449(5)
			Sr3/Y3−O1	(×4)	2.545(5)

[a] Corresponding to unit cell parameters and atomic coordinates from the synchrotron refinement.

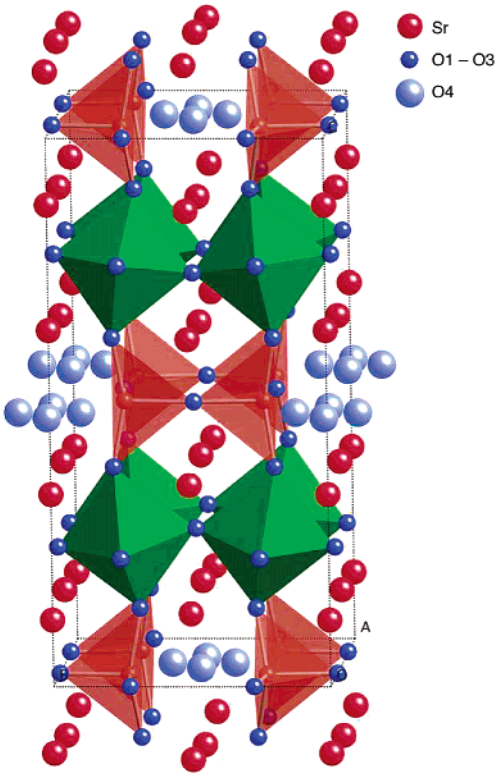

Figure 3. Crystal structure of $Sr_{0.7}Y_{0.3}CoO_{2.62}$. Layers with $Co2O_6$ octahedra alternate with oxygen-deficient layers containing the Co1, O3, and O4 atoms. The O4 site has an occupancy factor of $^1/_4$ and only one of the four adjacent positions of O4 is locally occupied.

were described by a Thompson modified pseudo-Voigt function. The refined value of the thermal parameter for the Co2 atom was slightly negative, −0.1(2) Å^2, for the neutron data set, and this parameter was therefore fixed to a physically reasonable value of 0.5 Å^2 in the final refinement. The R_I value increased thereby from 0.033 to 0.035, but the atomic coordinates remained the same within 1 esd. Observed and calculated patterns are shown in Figures 1 and 2. In the neutron pattern, the (112) reflection, marked with (∗) in Figure 1, has a notably lower calculated intensity than the observed one. We have no explanation for this discrepancy, which remained present in all the later described alternative structure models tried; it may coincide with a weak impurity peak. Crystal and refinement data for the two sets of data are given in Table 1 and the corresponding atomic coordinates in Table 2. In Table 3, selected interatomic distances are given, corresponding to the, comparatively better determined, atomic coordinates obtained from the synchrotron data.

The crystal structure of $Sr_{0.7}Y_{0.3}CoO_{2.62}$ is illustrated in Figure 3. It contains layers of tilted CoO_6 octahedra that alternate with oxygen-deficient layers containing the Co1 atoms. The O atoms in the oxygen-deficient layers are partially disordered in the structure model with the O4 atom distributed over four closely situated sites with a site occupancy factor of 0.25. The oxygen content in the model corresponds to an $ABO_{2.625}$ stoichiometry, in agreement with that experimentally determined by iodometric titration. Refinement of the occupancy using neutron powder diffraction data resulted in the value 0.23(1). The O atom disorder in the oxygen-deficient layers is discussed in more detail below.

Alternative tetragonal space groups with lower symmetries were also tested. Since neutron diffraction is much more sensitive than X-ray diffraction for oxygen atom positions, these refinements were made using only the NPD data. The refined thermal parameter for the Co2 atom was, as for the refinement in *I*4/*mmm*, negative for all models tested and this parameter was subsequently fixed to 0.5 Å^2 in the final stages of all the refinements. Structure models in the subgroups of *I*4/*mmm* did not result in significantly improved fits, despite the increased number of positional parameters used to describe the structure. Refinements in $I\bar{4}$ and

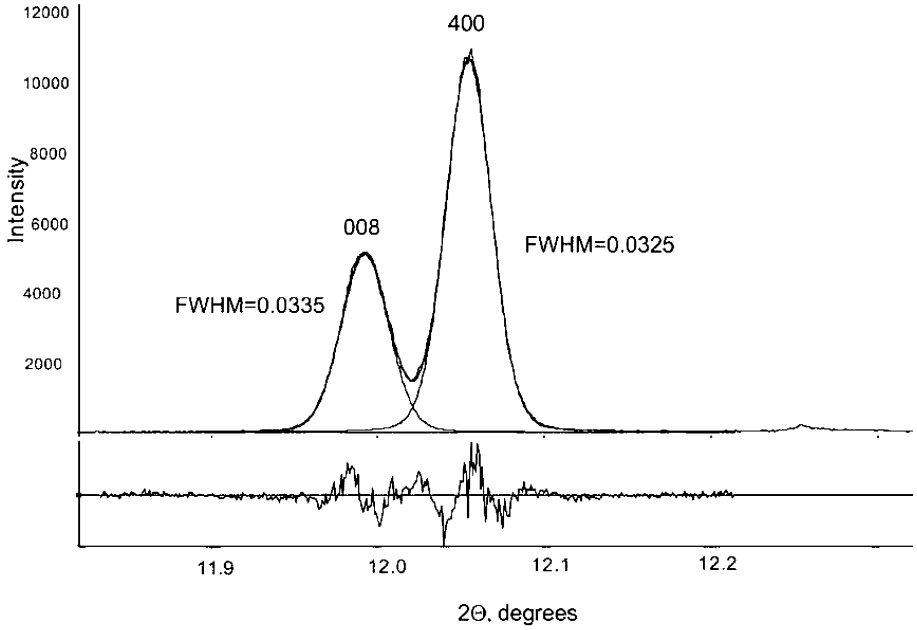

Figure 4. 008 and 400 Bragg reflections in the synchrotron powder pattern for $Sr_{0.7}Y_{0.3}CoO_{2.62}$. The similarity of their full-widths at half-maximum height (fwhm) shows that there is no indication of an orthorhombic distortion of the tetragonal unit cell in the powder data.

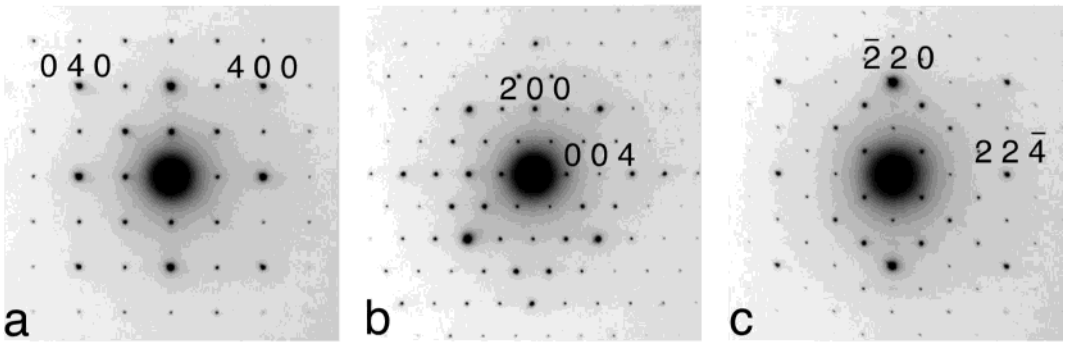

Figure 5. Selected area electron diffraction patterns of $Sr_{0.7}Y_{0.3}CoO_{2.62}$ crystallites, viewed along (a) [001], (b) [010], and (c) [111]. The reflection conditions agree with the *I*4/*mmm* symmetry used in the structure refinements.

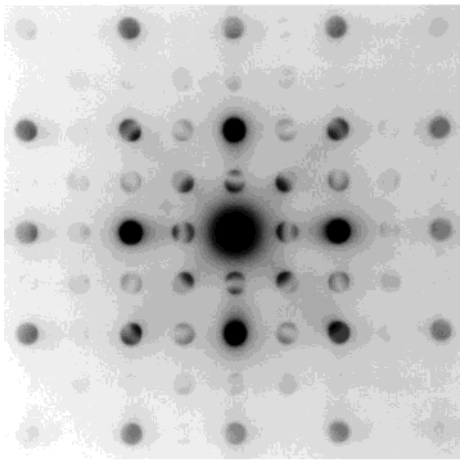

Figure 6. Microdiffraction pattern of $Sr_{0.7}Y_{0.3}CoO_{2.62}$, viewed along [001]. The 4*mm* symmetry of the pattern is in agreement with the space group *I*4/*mmm*,

*I*4 were unstable and unsatisfactory. In $I\bar{4}2m$, $I\bar{4}m2$, *I*4*mm*, and *I*4/*m*, the refinements yielded both low *R* values and reasonable thermal parameters. However, in $I\bar{4}2m$ and *I*4*mm*, unreasonably short Co−O distances were obtained, and in $I\bar{4}m2$ substantially increased esd's for the thermal parameters of the atoms corresponding to Sr2/Y2 resulted. The refinement in *I*4/*m* yielded a credible structure model, and *R* factors similar to those in *I*4/*mmm*, with five additional variable structural parameters. The derived atomic positions were, however, within error identical to those in *I*4/*mmm*, but with significantly higher esd's. The *I*4/*mmm* structure model is thus preferred since it agrees well with the experimental data and requires the least number of refinable structure parameters.

The split position of the O4 atom in the oxygen-deficient layers cannot be avoided in any tetragonal space group because of the presence of a 4-fold axis. Structure models with corresponding O atom sites that are ordered and fully occupied are, however, possible if the space group symmetry is lowered to orthorhombic, for example, in *Imm*2. Such models were tested, but yielded no improvement in fit. The possibility of a local order of the O atoms that has symmetry lower than tetragonal will be discussed later. Here, it can be noted that the synchrotron powder pattern shows no indication of an orthorhombic distortion of the unit cell. This is illustrated in Figure 4, where the reflections 040 and 008 are seen to have the same width at half-maximum height. There is thus no evidence in the powder diffraction data for an orthorhombic distortion.

Electron Microscopy. Selected area ED zone-axis patterns (ZAPs) were in full agreement with the tetragonal unit cell found by powder diffraction for many of the crystallites investigated. In these, there were no additional reflection conditions other than those of an I-centered Bravais lattice. ED patterns along [001], [010], and [111] are shown in Figure 5. The presence of a 4-fold axis was also supported by microdiffraction patterns, such as that shown in Figure 6. However, superstructure reflections and streaking were observed in some other crystallites, indicating further local order. The intensities varied from weak and diffuse to strong and distinct, both within and between crystallites. To explore their distribution in reciprocal space, a number of ED patterns were recorded in different tilt series. One such series, with the tilt around the *c*-axis, is shown in Figure 7. Superstructure reflections can be seen in the [001], [130], and [110] ED-ZAPs but not in those along

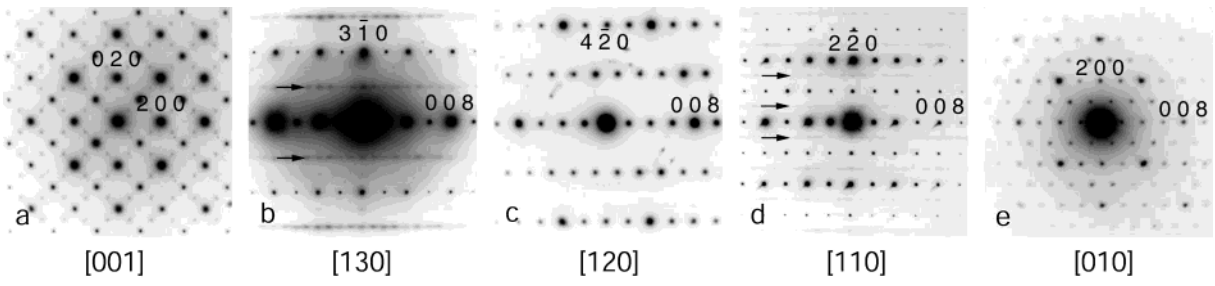

Figure 7. Selected area electron diffraction patterns of $Sr_{0.7}Y_{0.3}CoO_{2.62}$ in a tilt series around [010]. (a) Along [001]. There are satellite reflections at $^1/_2\langle 110\rangle$, indicating a doubling of at least one of the tetragonal *a* or *b* axis. (b) Along [130]. There are rows of superstructure reflections at $^1/_2 \pm \langle 310\rangle$, some of them violating the reflection condition $h + k + l = 2n$ for a body-centered cell. (c) Along [120]. There are no superstructure reflections observed. (d) Along [110]. There are rows of superstructure reflections along 00*l* at $^1/_2 \pm \langle 220\rangle$. The presence of superstructure reflections with $l = 2n + 1$ are not compatible with the body-centered unit cell. (e) Along [010]. No superstructure reflections observed.

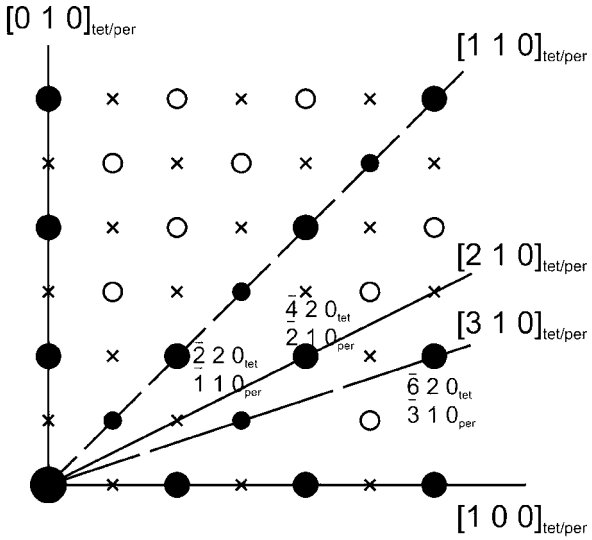

Figure 8. Schematic drawing of the reciprocal lattice made to illustrate the position of the superstructure reflections. Lattice points that correspond to the perovskite sublattice, tetragonal lattice, and superlattice are shown as large, medium, and small circles, respectively. The unit cell is indicated.

[010] or [120]. In the [001] ED-ZAP there are superstructure reflections at $G = {}^1/_2 \pm [110]$ and $G = {}^1/_2 \pm [1\bar{1}0]$ but not of the kind $G = {}^1/_2 \pm [100]$. This is also in agreement with the absence of superstructure reflections in the [100] ED-ZAP. In the [130] and [110] ED-ZAPs there are also superstructure reflections with $h + k + l \neq 2n$, which thus violates the body-centered symmetry. Distinct superstructure reflections were frequently also observed in [111] ED-ZAPs.

The superstructure reflections cannot be described with a larger tetragonal unit cell with $a = b = 2 \times \sqrt{2}\cdot a_p$ and $c = 4\cdot a_p$ because of the absence of superstructure reflections $G = \pm{}^1/_2[110]$. It is, however, possible to account for them by a twinned orthorhombic unit cell with $a = 2 \times \sqrt{2}\cdot a_p$, $b = \sqrt{2} \times a_p$, and $c = 4\cdot a_p$. The relation, in reciprocal space, between this cell and the tetragonal one is shown in Figure 8. A detailed model of the superstructure is, however, difficult to establish since, as noted above, the superstructure reflections are not observable in neutron or X-ray powder patterns.

It should be emphasized that superstructure reflections or streaking was never observed in ⟨100⟩ ED-ZAPs or in Fourier transforms of the corresponding HREM images. A HREM image of a crystallite viewed along [010] is shown in Figure 9. A fast-Fourier transform (FFT) and a Fourier filtered image of the encircled area is inserted. The latter is in good agreement with a simulated HREM image, using the coordinates in Table 3.

The HREM images of crystallites viewed along [001] (see Figure 10) exhibited lattice fringes corresponding to the perovskite sublattice and the {110} planes in the tetragonal unit cell. At a closer look 11.5-Å fringes, which correspond to the superstructure reflections discussed above, is discernible in different domains. A FFT image of such an area is encircled in Figure 10. In the FFT it can be seen that the superstructure reflections only appear in one of the (110) directions. This agrees with the notion of a local structure with the orthorhombic supercell $a = 2 \times \sqrt{2}\cdot a_p$, $b = \sqrt{2} \times a_p$, and $c = 4\cdot a_p$.

Discussion

The crystal structure of $Sr_{0.7}Y_{0.3}CoO_{2.62}$, illustrated in Figure 3, exhibits a new type of ordering of oxygen vacancies, with octahedral layers separated by oxygen-deficient layers with a partially disordered distribution of oxygen vacancies. The $Co2O_6$ octahedron is axially distorted, with four shorter equatorial distances, $d_{Co2-O1} = 1.9122(2)$ Å, and two longer axial distances, $d_{Co2-O2} = 2.076(3)$ Å. An analogous elongation of octa-

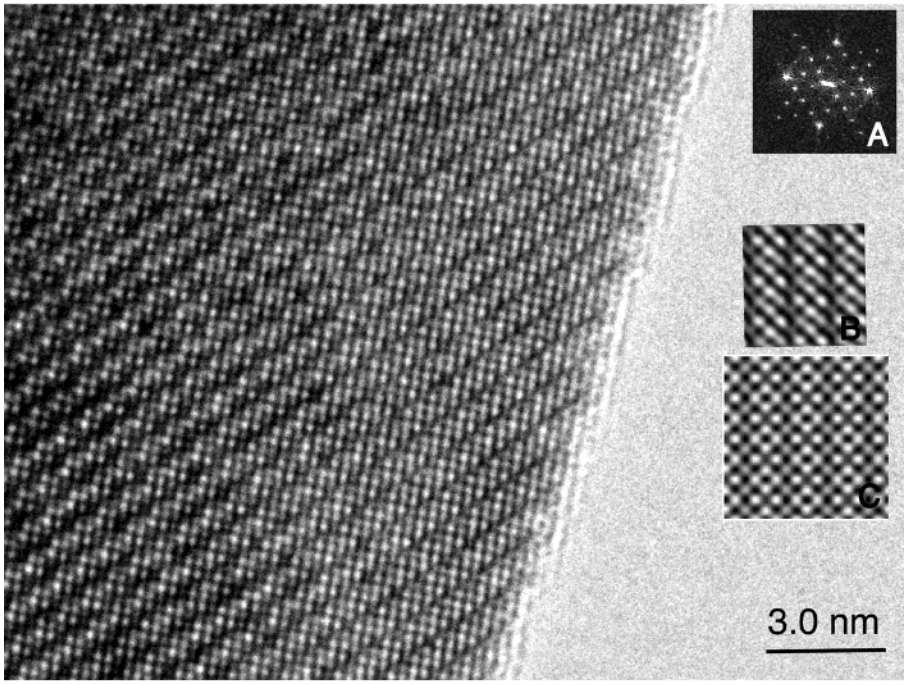

Figure 9. HREM image of $Sr_{0.7}Y_{0.3}CoO_{2.62}$ recorded along [010]. (A) A FFT pattern of an area close to the edge of the crystallite. (B) Fourier filtered image. (C) Simulated HREM image (defocus −300 Å, thickness 20 Å).

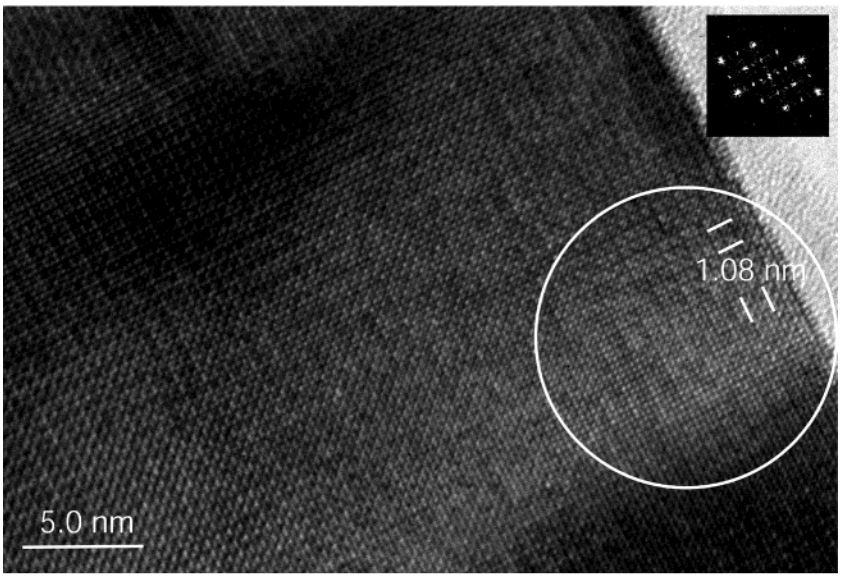

Figure 10. HREM image of $Sr_{0.7}Y_{0.3}CoO_{2.62}$ recorded along [001]. FFT pattern of the encircled area is the inset. Superstructure reflections along ⟨110⟩ can be seen in the FFT pattern. The corresponding repetition distances are marked in the HREM image.

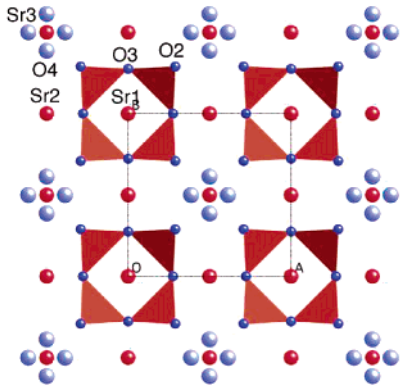

Figure 11. Structure drawing of $Sr_{0.3}Y_{0.7}CoO_{2.62}$ showing the layer with partial disordered oxygen (O4) at $z = 0.0$. Co1 polyhedron is drawn as tetrahedra. Sr1, Sr2, and Sr3 atoms at $z \approx 1/8$ are shown for clarity.

hedra is observed for oxides with the brownmillerite structure, for example, Sr_2MnGaO_5.[24] The cause of it has been attributed to the octahedra in different layers being connected via tetrahedra.[25] This explanation is equally valid for the case of $Sr_{0.7}Y_{0.3}CoO_{2.62}$. BVS calculations based on the bond valence parameter for Co^{3+} taken from ref 26 and interatomic distances from Table 3 showed valences quite close to the expected values: for Co2 the valence is 3.0 and the Co1 valence is 2.7.

The CoO_6 octahedra are rotated around the *a* and *b* axis. The tilting scheme according to Glazers notation would be $a^+a^+c^0$. This is different from what is found for brownmillerites, which have $a^-b^-c^0$. The tilting of the octahedra gives rise to three types of oxygen polyhedra around the Sr/Y atoms. The distance $d_{Sr3/Y3-O1} = 2.312(3)$ Å is quite short for a Sr−O bond, indicating

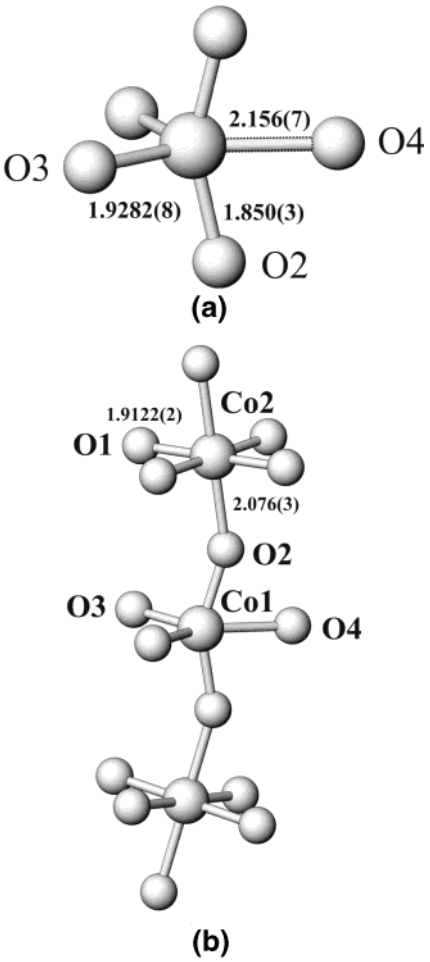

Figure 12. (a) Polyhedron of Co1 atom in the structure, which can be described as a tetrahedron with one additional oxygen atom O4 at the longest distance. (b) Connection of the $Co1O_{4+1}$ polyhedra with $Co2O_6$ octahedra from neighboring layers.

that the Sr3/Y3 position is preferentially occupied by Y. The powder diffraction data, however, give very little information in this respect since not only the X-ray scattering powers are very similar for Sr ($Z = 39$) and Y ($Z = 40$) but so are also the neutron scattering

(24) Abakumov, A. M.; Rozova, M. G.; Pavlyuk, B. Ph.; Lobanov, M. V.; Antipov, E. V.; Lebedev, O. I.; van Tendeloo, G.; Ignatchik, O. L.; Ovtchenkov, E. A.; Koksharov, Yu. A.; Vasilév, A. N. *J. Solid. State. Chem.* **2001**, *160*, 353.

(25) Lindberg, F.; Istomin, S. Ya.; Berastegui, P.; Svensson, G.; Kazakov, S. M.; Antipov, E. V. *J. Solid State Chem.* **2003**, *173*, 395.

(26) Brese, N. E.; O'Keeffe, M. *Acta Crystallogr.* **1991**, *B47*, 192.

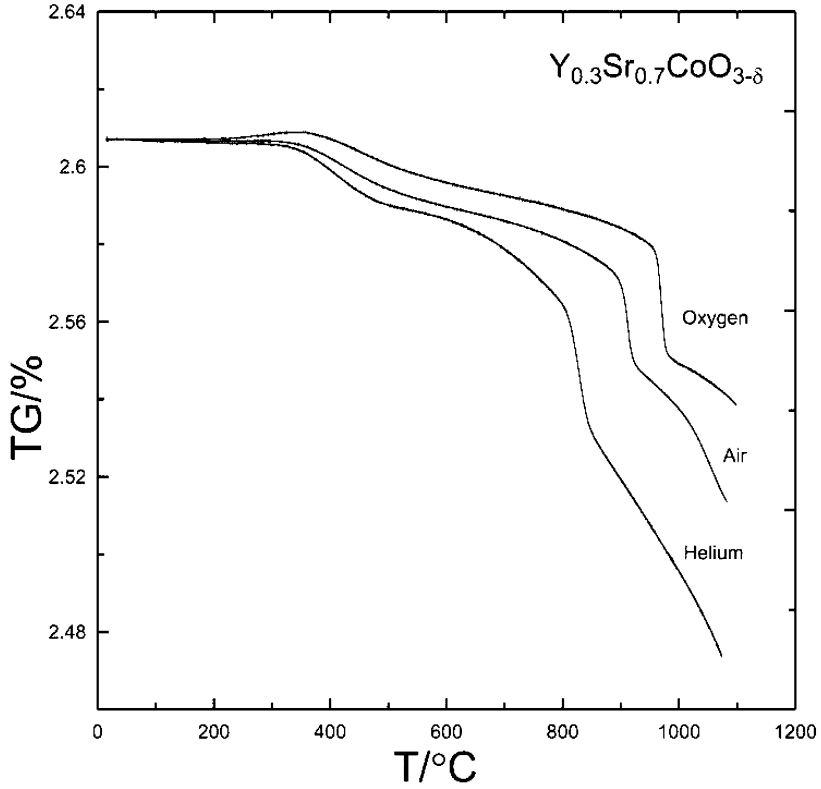

Figure 13. TG curves for $Sr_{0.7}Y_{0.3}CoO_{2.62}$ samples in oxygen, air, and helium. Note only a slight increase of the oxygen content in O_2.

lengths, 0.702 barns for Sr and 0.775 barns for Y.[27] A refinement of the Sr/Y atom site occupancies, using the NPD data, indicated in fact that the Sr3/Y3 position is preferentially occupied by Y atoms, but the refined values had large esd's. The presence of Y^{3+} in the Sr3/Y3 is supported by bond-valence sum calculations where Sr1 and Sr2 calculated using the parameters for Sr^{2+} have BVS's of 2.1 and 1.9, respectively, while it is 3.1 for Sr3/Y calculated using the parameter for Y^{3+}. To check the possibility of A-cation ordering, the isostructural compound $Sr_{0.7}Ho_{0.3}CoO_{2.62}$ containing Ho^{3+} (Z = 67), which has an ionic radius close to Y^{3+} ($r(Y^{3+}) = 1.02$ Å, $r(Ho^{3+}) = 1.01$ Å, CN = 8[28]) was prepared. Refinement of the crystal structure of $Sr_{0.7}Ho_{0.3}CoO_{2.62}$ using X-ray diffraction data indicate that the Sr3/Ho3 site is preferentially occupied by Ho atoms. Detailed structure studies of the compounds $Sr_{1-x}Ln_xCoO_{2.62}$, Ln = Eu−Ho, is in progress and will be reported elsewhere.

The atom arrangement in the oxygen-deficient layer, at $z = 0$, is illustrated in Figure 11. It has to be kept in mind here that only one of the four adjacent, partially occupied, O4 positions can be locally occupied because of their close proximity. The Co1 atoms are tetrahedrally coordinated by O2 and O3 atoms. The tetrahedra are arranged in clusters of four, with each tetrahedra sharing its two O3 atoms with adjacent tetrahedra. The local occupancy of one of the four split O4 positions effects a five-coordination for two of the four Co1 atoms in each layer. The resulting coordination polyhedron for the five-coordinated Co atoms is illustrated in Figure 12a. It is irregular and may alternatively be described as a distorted square pyramid or as a distorted trigonal bipyramid. The latter designation will be used here. The connection of the trigonal bipyramids with the octahedra in neighboring layers is shown in Figure 12b. There are accordingly an equal number of tetrahedra and trigonal bipyramids in the oxygen-deficient layers. The distances from Co1 to the O2 and O3 atoms are similar to previously reported ones for Co^{3+} in tetrahedra.[25]

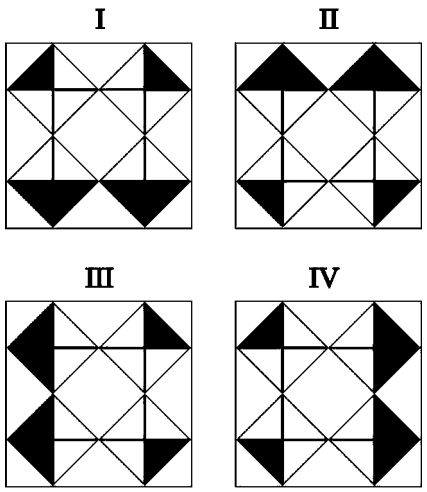

Figure 14. Four unique variants of ordering of the oxygen vacancies in the layers of the structure of $Sr_{0.7}Y_{0.3}CoO_{2.62}$. Note that the tetragonal structure can be described as a mixture of all four variants. The model of the structure in *Immm* represents a mixture of variants I and II or III and IV. The structure model in *Imm*2 depicts only one unique variant.

Thermogravimetric study (TG) of $Sr_{0.7}Y_{0.3}CoO_{2.62}$ in an oxygen atmosphere showed that the oxygen content of the phase is almost constant at 2.62 as only a slight weight increase is observed with a maximum at 325 °C (Figure 13). The same behavior was observed for the

(27) Sears, V. F. *Neutron News* **1992**, *3*, 26.
(28) Shannon, R. D. *Acta Crystallogr.* **1972**, *A32*, 258.

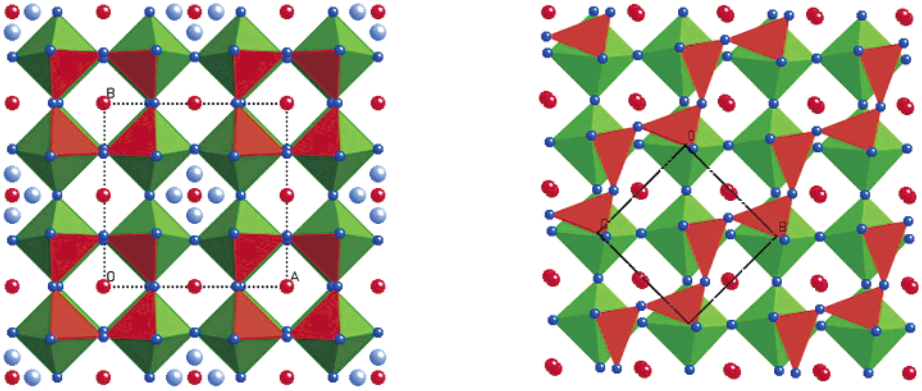

Figure 15. Structure of the vacant layers in the brownmillerite ($Sr_2Co_2O_5$) and in $Sr_{0.7}Y_{0.3}CoO_{2.62}$. Only one position in the structure of $Sr_{0.7}Y_{0.3}CoO_{2.62}$ marked with blue circles is occupied per unit cell.

isostructural $Sr_{0.7}Ho_{0.3}CoO_{2.62}$. The almost constant upper limit of the oxygen composition is in agreement with the structure since additional oxygen in the disordered layer requires substantial rearrangement of the structure. The loss of oxygen above 400 °C is easier to explain since the O4 oxygen is weakly bounded. The bond-valence sum for O4 is 1.2. A complete removal of the O4 oxygen from the structure corresponds to an oxygen content of 2.5. TG in oxygen, air, and helium showed that oxygen content rapidly decreases with increasing temperature and at about 1000 °C in helium it approaches 2.5 (Figure 13).

In the derived *I*4/*mmm* structure model, there are 42 oxygen atoms in the unit cell, in agreement with the determined oxygen content, in comparison with 48 oxygen atoms for a completely filled anion sublattice. Taking into account that vacancies are located in every second layer only, there are three oxygen vacancies within the unit cell in each oxygen-deficient layer. Consequently, there are two trigonal bipyramids and two tetrahedra per such layer. Four ways to distribute these locally in the tetragonal cell are shown in Figure 14. None of the variants alone are compatible with the *I*4/*mmm* symmetry. Each particular case, for example, I in Figure 14, can, however, be described using the orthorhombic space group *Imm*2. A structure model for an average structure of two of the variants, for example, I and II, can furthermore be described in *Immm*. The *I*4/*mmm* model accordingly describes an average structure of local distributions of all four variants in equal amounts. The supercell $a = 2 \times \sqrt{2} \times a_p$, $b = \sqrt{2} \times a_p$, and $c = 4 \times a_p$ found in the ED pattern cannot be described by ordering of the O4 atoms. It is therefore associated with rearrangement of all oxygen atoms in that layer.

In comparison with the brownmillerite structure found for $SrCoO_{2.5}$, in $Sr_{0.7}Y_{0.3}CoO_{2.62}$ there is one additional oxygen atom per layer with $2a_p \times 2a_p$ dimension. An illustration of the tetrahedral layer in the ordered brownmillerite structure, together with the oxygen-deficient layer for $Sr_{0.7}Y_{0.3}CoO_{2.62}$, is given in Figure 15. The figure shows that the distribution of oxygen vacancies is quite different in the two structures and that the latter cannot be directly derived from the brownmillerite structure. Another distinct difference between the two structures discussed above is the way in which the octahedra are tilted. Such differences in the structures can be explained taking into account that the driving force of the formation of the $Sr_{0.7}Y_{0.3}CoO_{2.62}$ phase may be ordering of the Y^{3+} and Sr^{2+}, which leads in turn to the ordering of the oxygen vacancies.

Concluding Remarks

The structure of $Sr_{0.7}Y_{0.3}CoO_{2.62}$ represents a new type of layered ordering of oxygen vacancies in oxygen-deficient perovskites. The $ABO_{2.625}$ structure is similar to the $ABO_{2.5}$ brownmillerite structure in that the oxygen vacancies are found in alternating B atom layers, as opposed to related structures with higher oxygen contents, for example, $Sr_4Fe_4O_{11}$ ($ABO_{2.75}$) and $Sr_8Fe_8O_{23}$ ($ABO_{2.875}$),[9] in which the vacancies are distributed more uniformly.

Acknowledgment. We acknowledge the European Synchrotron Radiation Facility for provision of synchrotron radiation facilities and we would like to thank Dr. A. C. McLaughlin and H. Nowell for using beamline ID31 and collecting the data. Håkan Rundlöf at NFL Studsvik is thanked for collecting NPD data. We also thank the Swedish research council and the Royal Swedish Academy of Sciences (KVA) for financial support. This work was partially supported by RFBR (03-02-32990). Acknowledgment is made to the donors of the American Chemical Society Petroleum Research Fund for support of this research (PRF ACS 38459-AC5). S.Ya.I. acknowledges the Scientific Council of MSU and E.V.A. acknowledges the Russian Science Support Fund.

Supporting Information Available: X-ray crystallographic data for $Sr_{0.7}Y_{0.3}CoO_{2.62}$ (CIF). This material is available free of charge via the Internet at http://pubs.acs.org.

CM034263E